JOURNAL OF GEOPHYSICAL RESEARCH

Supporting Information for "Rheologic constraints on the upper mantle from five years of postseismic deformation following the El Mayor-Cucapah earthquake"

Trever T. Hines, ¹ Eric A. Hetland, ¹

Contents of this file

1. Figures S1 to S4 $\,$

Introduction

Figures S1 and S2 provide additional information about the inversion in Section 3.2 of the main text. Figures S3 and S4 show the predicted displacements, which have been decomposed into elastic and viscoelastic components, for the preferred model from Section 3.3.

Corresponding author: T. T. Hines, Department of Earth and Environmental Sciences, University of Michigan, 2534 C. C. Little Building, 1100 North University Avenue, Ann Arbor, MI 48109-1005. (hinest@umich.edu)

¹Department of Earth and Environmental

Sciences, University of Michigan, Ann

Arbor, Michigan, USA.

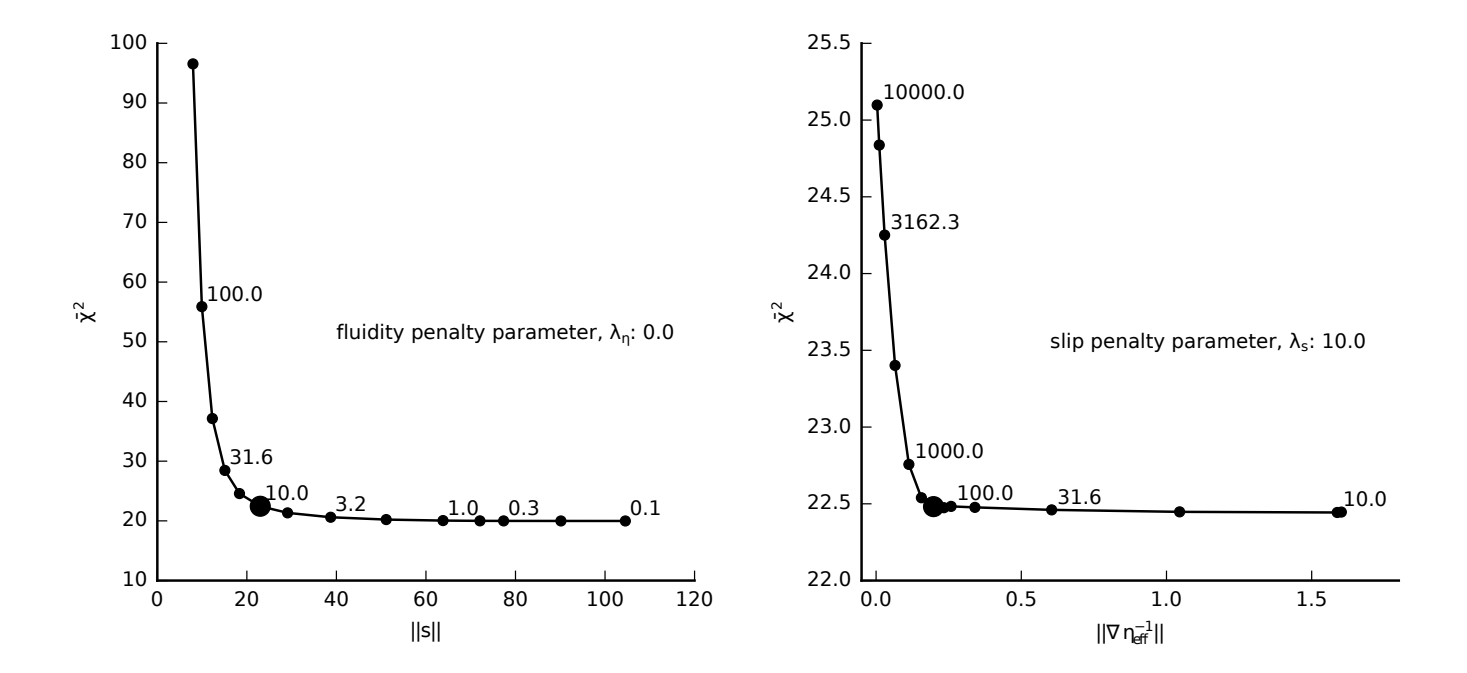


Figure S1. Trade-off curves used to determine the damping parameters λ_s and λ_{η} in eq. (15) of the main text. The left panel shows the trade-off curve for the fault slip penalty parameter, λ_s . We pick λ_s while keeping the penalty parameter for fluidity, λ_{η} , fixed at zero. The right panel shows the trade of curve for selecting λ_{η} , where we fix λ_s at the chosen value from the left panel. Chosen values are indicated with the larger marker. When picking λ_s , we try to find a good balance between the mean chi-squared value, $\bar{\chi}^2$, and the size of the slip parameters, ||s||. Our choice of λ_{η} is a balance between $\bar{\chi}^2$ and the size of the Laplacian of fluidity, $||\nabla \eta_{\text{eff}}^{-1}||$.

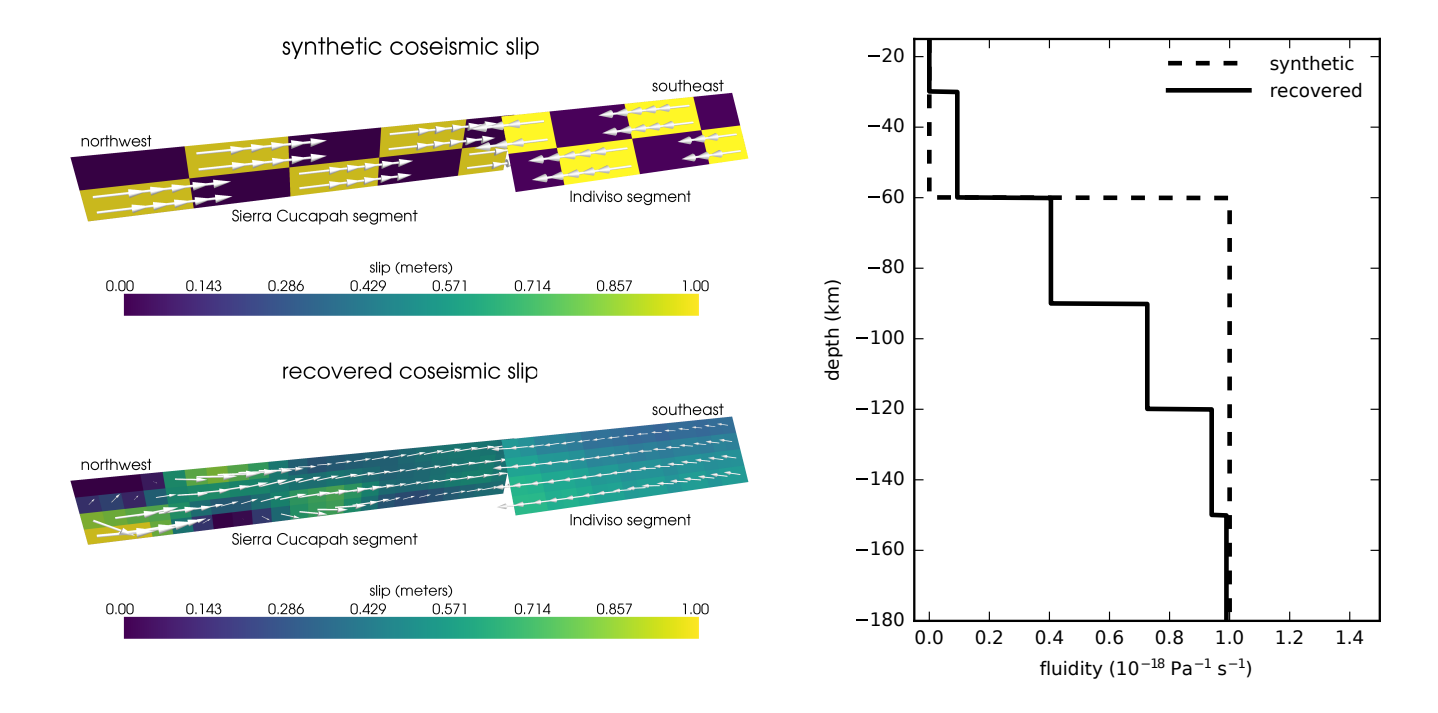


Figure S2. Checkerboard test used to assess the resolving power of the inversion in Section 3.2 of the main text. We create synthetic data at all of the GPS stations considered in this study by evaluating eq. (14) with the synthetic coseismic slip distribution and fluidity distributions. Our synthetic fluidity model has a jump from 0.0 to 10^{-18} Pa⁻¹ s⁻¹ at 60 km depth. Our synthetic slip model does not include afterslip, although we estimate afterslip along with coseismic slip and fluidity in this test. We estimate these values in the same way as described in the main text and we also use the same penalty parameters. We do not add any noise to our synthetic data so that the recovered model just indicates how much the regularization influences the solution. Note that our ability to recover slip decreases towards the southern end of the fault, farthest from the available data. Also note that the smoothing constraint on fluidity largely obscures the jump in the synthetic model.

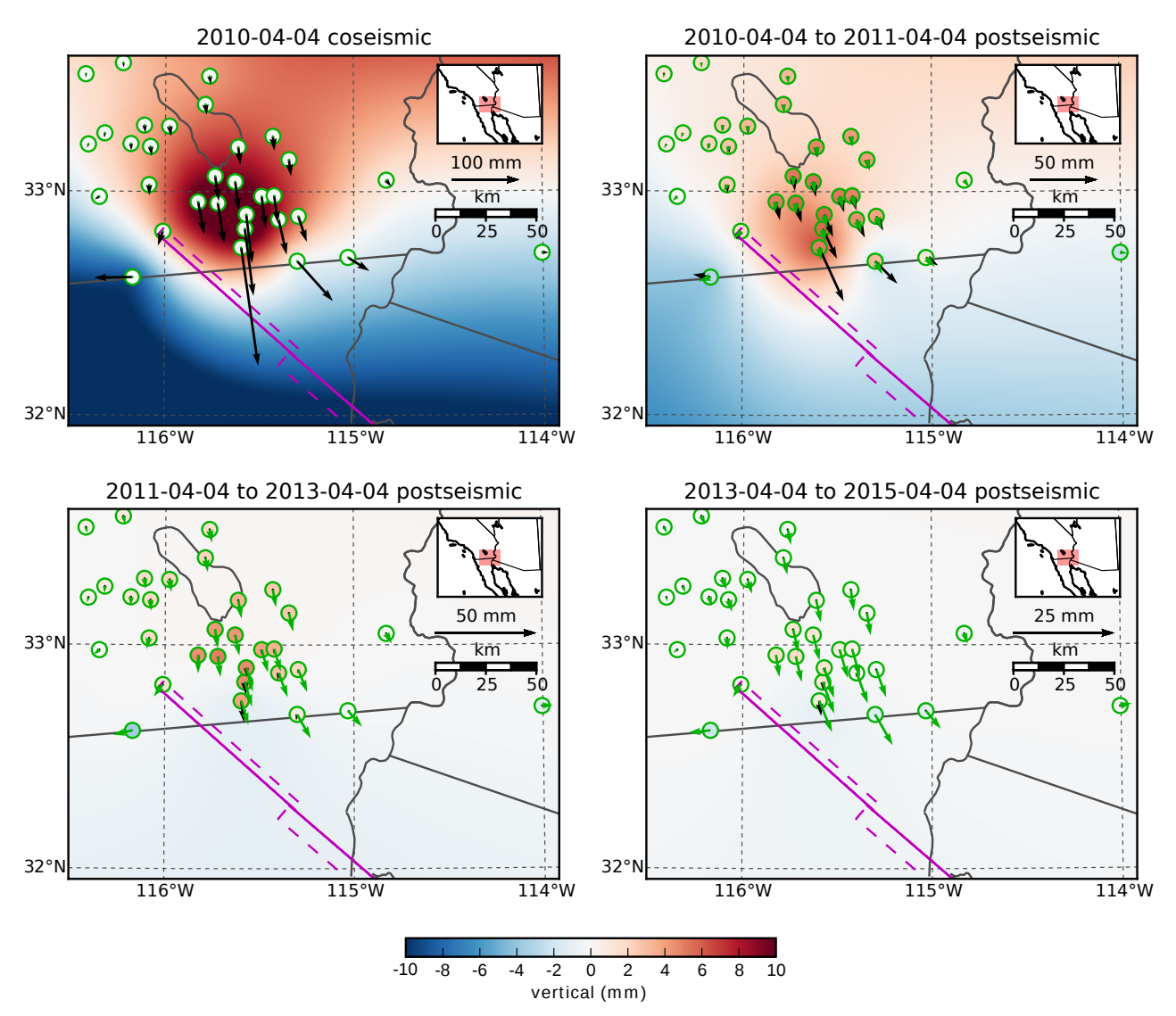


Figure S3. Elastic (black) and viscoelastic (green) components of the near-field predicted displacements for the preferred Zener model from Section 3.3. The vertical elastic component is shown as an interpolated field and the vertical viscoelastic components are shown within the green circles. The elastic and viscoelastic components are calculated from the first and second term in eq. (11). The elastic component can be interpreted as the displacements resulting from fault slip and the viscoelastic component can be interpreted as the displacement due to relaxation of stresses induces by the slip.

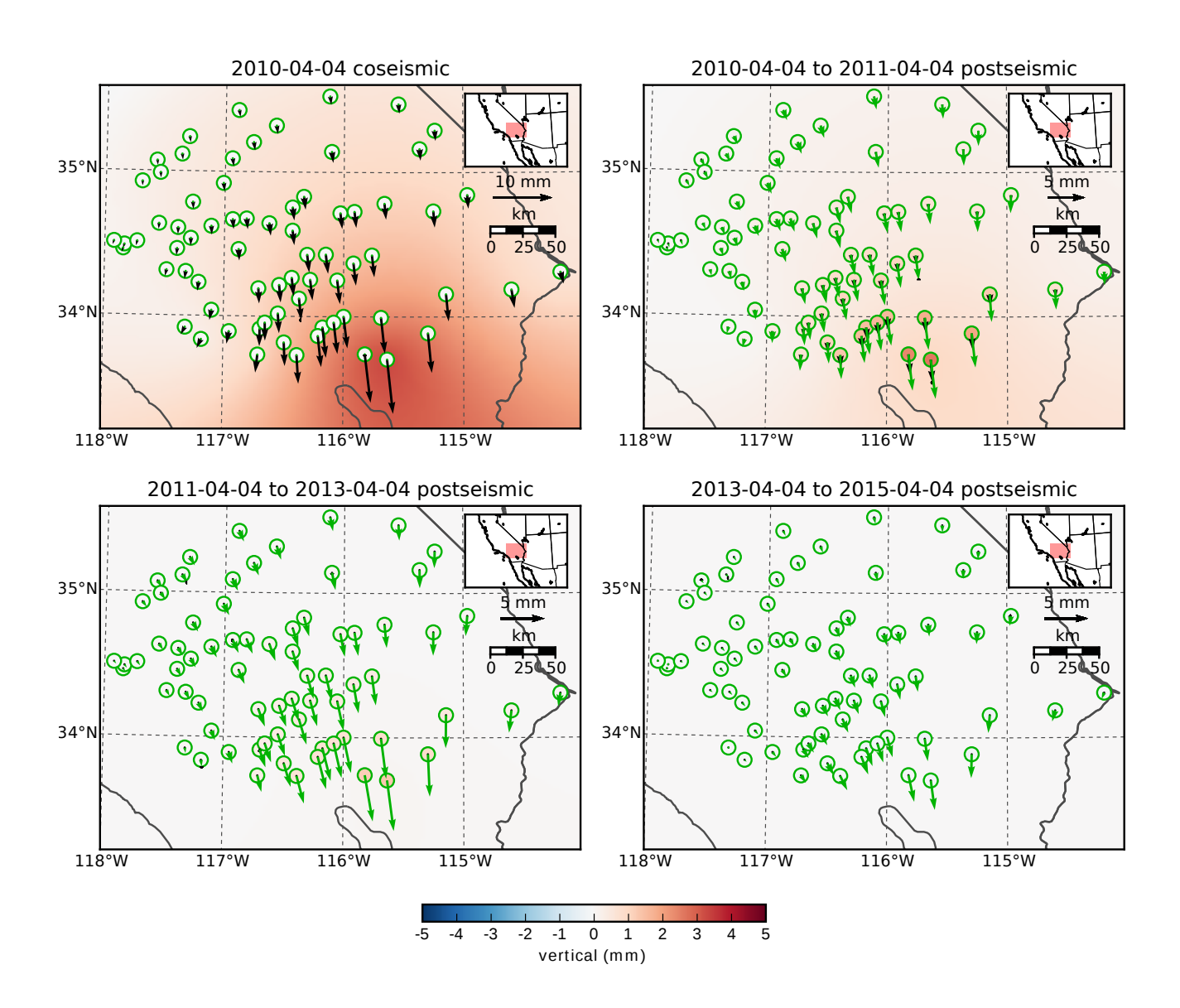


Figure S4. Same as figure S3 but for far-field stations.